Rare frustration of optical supercontinuum generation

D. R. Solli,[1,a)] C. Ropers,[1,2] and B. Jalali[1]
[1]*Department of Electrical Engineering, University of California, Los Angeles, Los Angeles, California 90095, USA*
[2]*Courant Research Center Nano-Spectroscopy and X-Ray Imaging, University of Göttingen, Germany*

(Received 6 February 2010; accepted 24 February 2010; published online 14 April 2010)

Recent work has shown that optical rogue waves, large bandwidth fluctuations following heavy-tailed statistics, can arise during spectral broadening by stochastic enhancement of nonlinearity. Here, we report the observation of a different form of extreme fluctuations in supercontinuum pulse trains: Pulses of unusually small spectral bandwidth following left-skewed heavy-tailed statistics. Displaying a pulse evolution strongly varying from that of large extremes in supercontinuum, these rogue events appear when spectral broadening is frustrated by competition between presolitonic features within the modulation-instability band. This suppression effect can also be externally induced with a weak control pulse. © *2010 American Institute of Physics*. [doi:10.1063/1.3374860]

Many dynamic, complex systems produce rare, extreme events, or outliers—rare instances of strongly atypical behavior. Although infrequent and short-lived, such anomalous events can have a defining influence on the long-term condition of the system. Financial volatility, pandemics, and freak ocean waves testify to the existence and impact of these unusual events. Their underlying statistics, heavy-tailed distributions, assign greater probabilities to anomalous events than normal distributions.[1,2] Heavy-tailed statistics arise when input fluctuations are mapped into a skewed output distribution by a nonlinear relationship.

Extreme events also appear within ultrafast phenomena; rare broadband pulses, optical rogue waves, can arise in nonlinear optical fiber during supercontinuum (SC) generation.[1,2] In other optical contexts, non-Gaussian statistics can arise in soliton-based communication systems,[3] beam filamentation,[4] Raman amplifiers,[5] and UV spectral broadening.[6] The observation of rare events in SC generation has implied analogies with other physical systems, and has proven useful for studying SC dependencies on input noise.

Here, we report the observation of small-amplitude extremes in SC generation, anomalous events corresponding to a rare frustration of spectral broadening. These events follow a left-skewed (reverse heavy-tailed) distribution, in which events far below the mean occur with small but non-negligible probability. Pulse-resolved measurements show that a small fraction of pulses experiences significantly less broadening than most, leading to rare gaps in the long-wavelength-filtered portion of the SC pulse train [cf. Fig. 1(a)]. As explained below, a stochastic depletion effect causes the SC generation process to be occasionally slowed.

Using real-time analog-to-digital converters, extreme SC spectra can be detected in a fast pulse series.[1] To produce SC, we inject near transform-limited pump pulses (1550 nm, 3 ps, and 25 MHz) from a mode-locked laser into 15 m of nonlinear optical fiber (dispersion: $\beta_2 = 1.13 \times 10^{-4}$ ps^2/m,

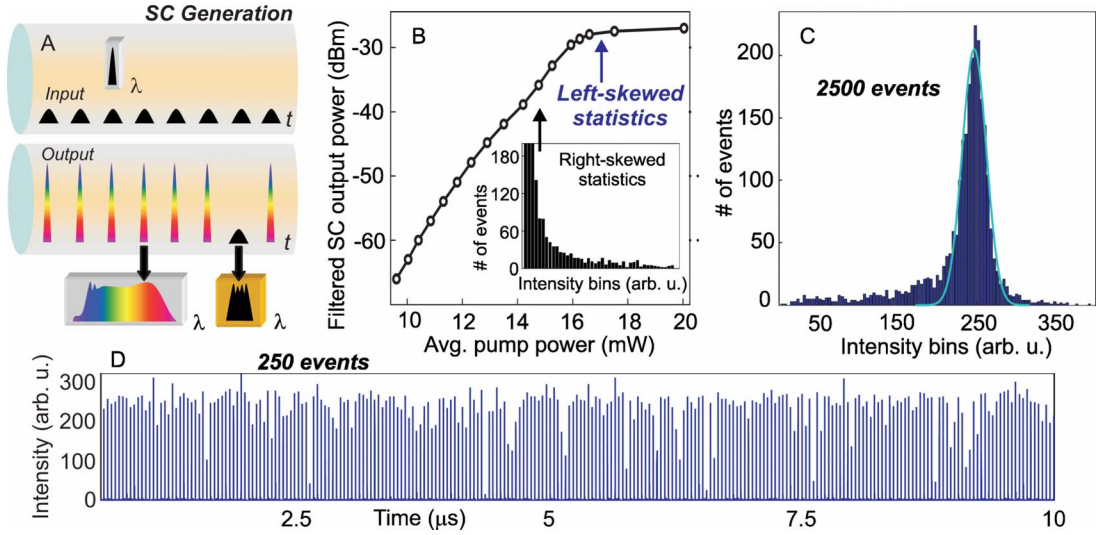

FIG. 1. (Color online) (a) Conceptual illustration of a narrowband extreme event in SC generation. (b) Experimental measurement of red-filtered SC output power vs average power of input pulse train. Right-skewed heavy-tailed statistics exist below threshold; left-skewed (reverse) heavy-tailed statistics appear above threshold. (c) Experimental observation of reverse-heavy-tailed statistics at the input power level labeled by the arrow in B. Gaussian is fit to the main portion of the distribution. (d) Filtered SC pulse train measured in real time.

a)Electronic mail: solli@ucla.edu.

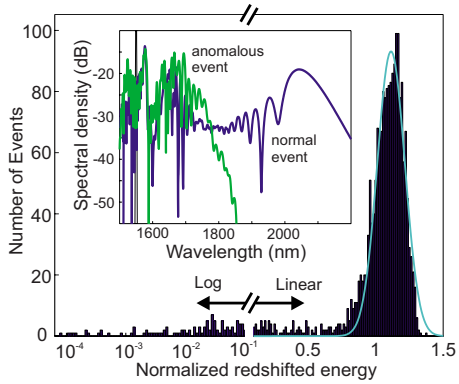

FIG. 2. (Color online) Reverse-heavy-tailed distribution from simulation of 2000 independent events (red-filtered energy). (P_0=210 W, $\varepsilon=4\times10^{-5}$) Gaussian is fit to the main portion of the distribution; a portion of the extreme tail is shown in log scale. Inset: Spectra of one anomalous (green) and one normal event (blue). Pump (input) spectrum also shown (black).

$\beta_3=6.48\times10^{-5}$ ps^3/m, nonlinear coefficient: $\gamma=10.66$ W^{-1} km^{-1}). At the fiber output, a spectral region redshifted from the input wavelength is selected with a red bandpass filter ($\lambda_0=1705$ nm, $\Delta\lambda=48$ nm). By applying the wavelength-time transformation technique to the output, the optical spectrum of each event can be sampled at multiple points. If spectrally resolved data are not required, the long-wavelength energy can be detected with a photodetector and ADC immediately after the filter.[1,2]

By measuring the time-averaged power passed by the filter, we determine the input power level needed to generate significant spectral broadening [cf. Fig. 1(b)]. For any redshifted filter position, this long-wavelength energy shows a threshold response to input power, saturating for larger input power levels. For a filter close to the modulation instability (MI) (Ref. 7) band, this threshold corresponds to the onset of soliton formation for the majority of noise-seeded events. Hence, this filter position allows for a sensitive discrimination of those events in which soliton fission is enhanced or frustrated. As previously reported, rogue waves appear below threshold. On the other hand, rare events that are relatively narrowband appear above threshold, and can be readily seen as rare gaps in the long-wavelength-selected portion of the SC pulse train [cf. Figs. 1(c) and 1(d)]. Time-averaged power measurements are insensitive to these events.

We also model this effect by solving the nonlinear Schrödinger equation (NLSE), which is widely used to study SC generation in fiber.[7,8] We include weak broadband stochastic perturbations in the temporal envelope of the Gaussian input field and simulate propagation in the nonlinear fiber for many independent events. For each event, the field is constructed as follows: $A(z=0,t)=\sqrt{P_0}e^{-(t-t_0)^2/\tau^2}\{1+\varepsilon[\mathrm{r}_1(t)+i\times\mathrm{r}_2(t)]\}$, where we have pulse duration τ, peak power P_0, and noise coefficient ε, and $\mathrm{r}_1(t)$, $\mathrm{r}_2(t)$ are selected at each time point from a standard normal distribution. The noise bandwidth is filtered to 30 THz about the pump.

Above the input power threshold, we find a left-skewed heavy-tailed distribution for the redshifted energy (cf. Fig. 2), as observed experimentally. We also examine these statistics as a function of the cutoff wavelength. The distribution has negative skew for a wide range of cutoff wavelengths. In each case, most events lie within a quasi-Gaussian portion of the distribution, with extreme events

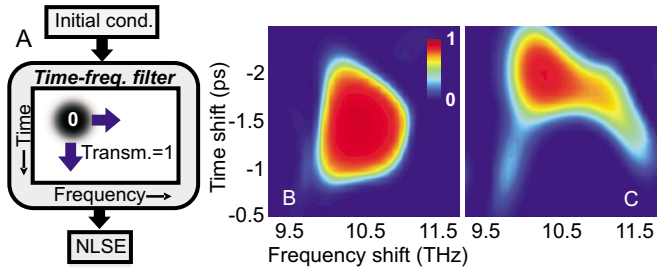

FIG. 3. (Color online) (a) A scanned time-frequency filter (Gaussian profile, $\Delta t=1$ ps; $\Delta f=1$ THz; center position specified by x and y axes) is applied to the input noise of two simulated anomalous events; the NLSE is then solved. [(b) and (c)] Redshifted energy (>1870 nm) at the fiber output for each filter position and two separate anomalous (frustrated broadening) events.

appearing within an extended tail. For longer cutoff wavelengths, the minimum events within the long tail become increasingly extreme relative to the mean. For these calculations, we approximate the Raman gain with a linear detuning dependence;[7] using the full Raman response function with spontaneous emission may slightly alter the extreme tails of the distribution. However, the basic features and pulse dynamics, as observed experimentally, should persist.

Large spectral broadening factors are obtained when intense narrowband pulses are injected into a nonlinear fiber at its zero-dispersion wavelength.[8] MI initially amplifies certain components of the ambient noise, creating spectral sidebands and leading to soliton breakup of the pulse;[9] the Raman self-frequency shift then causes a progressive redshift. Since the MI sidebands must build to a critical level to trigger fission, the redshifted energy displays a threshold response to input power. The pulse-to-pulse amplitude stability and phase coherence are usually lost because MI is seeded by noise.[8,10–13]

In this process, the input pulse power and noise level are both important parameters. However, the mechanism is specifically sensitive only to noise with frequency content and timing capable of seeding MI;[1,2] below threshold, a random surplus in this noise component can produce a rare redshifted soliton or rogue wave.[1,14] This process can also be exploited to influence SC generation with an external signal[14–16] or feedback loop;[17] stimulating the process with a controlled signal, for example, results in improved stability.[14,15]

When the input power and noise level should be sufficient to produce a broadband output spectrum, narrowband events still arise. An input-output comparison from many simulated events reveals that the narrowband extremes are not generally correlated with reductions in input noise components. The lack of a correlation indicates that the narrowband events are not a simple corollary of the rogue waves observed below threshold, for which unusually broadband spectra correlate with a specific surplus in noise seeding MI.

To study this mechanism in greater detail, we systematically delete different noise components from the initial conditions (ICs) with a time-frequency filter [cf. Fig. 3(a)]. By selectively removing specific components of the noise, we can determine each component's impact on broadening in the fiber. Performing the procedure for a raster of times and frequencies generates a map relating the noise to the SC bandwidth. For the rare, narrowband events, typical redshifted energy is produced if a small component of the input noise is *removed* [cf. Figs. 3(b) and 3(c)]. A redshifted soliton is present in the output time-frequency profile only when this

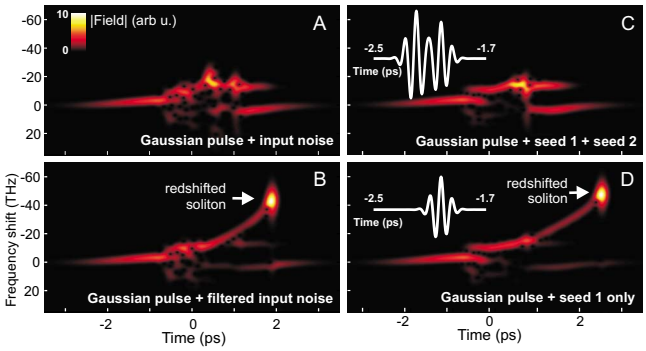

FIG. 4. (Color online) Windowed Fourier transforms of simulated fiber outputs for different initial conditions. (a) Anomalous event (Gaussian pulse+input noise). (b) Same event after removal of a noise component as shown in Fig. 3. (c) Noiseless Gaussian input+two interfering seed pulses. (d) Noiseless Gaussian input+single seed pulse.

noise component is deleted from the IC [cf. Figs. 4(a) and 4(b)]. Here, we observe that excluding a particular noise component accelerates spectral broadening in SC generation for some events.

In order to obtain a better understanding of the role of noise in the observed rare suppression of spectral broadening, we reduce the complexity of the problem by mimicking the random dynamics with controlled seed pulses. Previously, this approach has proven useful in studying the seeding process behind rogue waves.[14] Furthermore, induced MI has been previously explored for a variety of applications.[7] For example, it has been used to generate high-repetition rate pulse trains[18] and promote Raman soliton formation.[19] Here, we observe that a very weak signal can also delay SC generation by influencing MI.

While the characteristics of the normal events can be reproduced with a single seed pulse, the anomalous (suppressed broadening) events can be emulated by the application of at least two seeds to the pump. ICs suitable for seeded SC (Refs. 14 and 20) produce a redshifted soliton [cf. Fig. 4(d)] in a pulse structure strikingly similar to that of the anomalous IC after noise filtering. [cf. Fig. 4(b)]. Adding a second seed with a slightly different delay and frequency shift[20] results in an evolution [cf. Fig. 4(c)] that mirrors that of the anomalous ICs without noise filtering [cf. Fig. 4(a)]. In this situation, the additional pulse frustrates broadening. Addition of the second seed increases the temporal span of the modulation on the initial pump envelope [cf. Figs. 4(c) and 4(d), inset]; by studying the subsequent evolution in simulations, we find that this modulation evolves into two independent sharp features rather than just one. The two interfering seeds—each capable of stimulating SC individually—thus compete for the total MI gain, locally deplete the pump, and frustrate soliton fission.

Having observed that multiple seed features may compete for MI gain, we return to the noise-initiated SC to search for similar behavior. Indeed, a comparison of the pulse dynamics of normal and anomalous events shows that the latter generally exhibit the formation of multiple presolitonic features, while normal events usually contain one dominant sharp waveform [cf. Figs. 5(a) and 5(b)].

Additional features do not substantially delay soliton fission if they do not deplete the same portion of the pump envelope or if they coalesce at an early stage. An analysis of a large population of events shows that the anomalous events

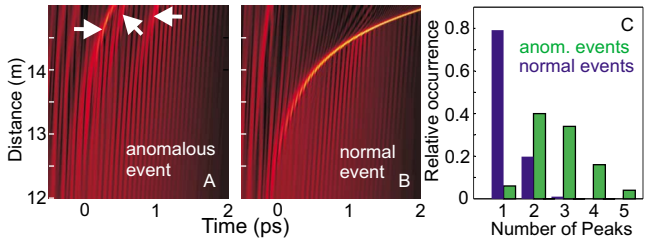

FIG. 5. (Color online) Propagation in the fiber of (a) an anomalous and (b) a normal event above the soliton fission threshold. Color scale illustrates the field magnitude (bright: Large magnitude). Arrows in (a) point to three presolitonic features. (c) Statistical analysis of the number of separate peaks above an arbitrary reference level in normal events (blue) and frustrated events (green, black outline) at the end of the fiber.

tend to have a greater number of sharp wavepackets than normal events [cf. Fig. 5(c)]. With sufficient propagation in a low-loss fiber, an anomalous event would eventually produce multiple redshifted solitons but this does not occur within the specified length.

In conclusion, we have observed rare frustration in optical SC generation above the soliton fission threshold. Above threshold, many noise components are capable of seeding soliton fission, saturating the process and generally making it less discriminative. Within this saturated regime, the anomalous events arise due to a rare and specific competition between presolitonic features seeded by the input noise. Such events can be reproduced with two or more seed pulses. This effect creates numerous possibilities for switching and coherent control of nonlinear broadening.

This work was supported by DARPA and NSF. C.R. acknowledges funding by the German Excellence Initiative (DFG-ZUK 45/1).

[1]D. R. Solli, C. Ropers, and B. Jalali, Nature (London) **450**, 1054 (2007).
[2]J. M. Dudley, G. Genty, and B. J. Eggleton, Opt. Express **16**, 3644 (2008).
[3]C. R. Menyuk, Opt. Lett. **20**, 285 (1995).
[4]J. Kasparian, P. Béjot, J.-P. Wolf, and J. M. Dudley, Opt. Express **17**, 12070 (2009).
[5]J. Chang, D. Baiocchi, J. Vas, and J. R. Thompson, Opt. Commun. **139**, 227 (1997).
[6]A. Aalto, G. Genty, and J. Toivonen, Opt. Express **18**, 1234 (2010).
[7]G. P. Agrawal, *Nonlinear Fiber Optics*, 4th ed. (Academic, New York, 2007).
[8]J. M. Dudley, G. Genty, and S. Coen, Rev. Mod. Phys. **78**, 1135 (2006).
[9]J. Herrmann, U. Griebner, N. Zhavoronkov, A. Husakou, D. Nickel, J. C. Knight, W. J. Wadsworth, P. St. J. Russell, and G. Korn, Phys. Rev. Lett. **88**, 173901 (2002).
[10]H. Kubota, K. R. Tamura, and M. Nakazawa, J. Opt. Soc. Am. B **16**, 2223 (1999).
[11]A. L. Gaeta, Opt. Lett. **27**, 924 (2002).
[12]K. L. Corwin, N. R. Newbury, J. M. Dudley, S. Coen, S. A. Diddams, K. Weber, and R. S. Windeler, Phys. Rev. Lett. **90**, 113904 (2003).
[13]F. Vanholsbeeck, S. Martin-Lopez, M. González-Herráez, and S. Coen, Opt. Express **13**, 6615 (2005).
[14]D. R. Solli, C. Ropers, and B. Jalali, Phys. Rev. Lett. **101**, 233902 (2008).
[15]G. Genty, J. M. Dudley, and B. J. Eggleton, Appl. Phys. B: Lasers Opt. **94**, 187 (2009).
[16]A. Efimov and A. J. Taylor, Opt. Express **16**, 5942 (2008).
[17]P. M. Moselund, M. H. Frosz, C. L. Thomsen, and O. Bang, Opt. Express **16**, 11954 (2008).
[18]K. Tai, A. Tomita, J. L. Jewell, and A. Hasegawa, Appl. Phys. Lett. **49**, 236 (1986).
[19]A. S. Gouveia-Neto, M. E. Faldon, and J. R. Taylor, Opt. Lett. **13**, 1029 (1988).
[20]Seed 1: Duration 200 fs, detuning −10 THz, delay −2 ps (relative to a noiseless Gaussian pump). Seed 2: −2.2 ps and −9.9 THz. Other parameter combinations can achieve similar effects.